ISSN 1813-3290, http://www.revist.ci

ELLIPTICAL CRACK UNDER ARBITRARILY APPLIED LOADINGS : DISLOCATION, CRACK-TIP STRESS AND CRACK EXTENSION FORCE

P.N.B. ANONGBA

Université F.H.B. de Cocody, U.F.R. Sciences des Structures de la Matière et de Technologie, 22 BP 582 Abidjan 22, Côte d'Ivoire

(reçu le 03 Novembre 2021 ; accepté le 28 Décembre 2021)

* Correspondance, e-mail : *anongba@gmail.com*

ABSTRACT

An elliptical crack of centre *O*, in an infinitely extended isotropic elastic medium stressed uniformly in an arbitrary manner at infinity, is the subject of the present study. The applied tension σ_{22}^{a} acts in the vertical x_2 - direction and the shears σ_{21}^{a} and σ_{23}^{a} act in the x_1 and x_3 directions, respectively. Poisson's normal stresses $-\nu\sigma_{22}^{a}$ (ν is Poisson's ratio) acting in the x_1 and x_3 directions are incorporated into the analysis. The crack is in the plane $(\pi) = Ox_1^{'}x_3^{'}$ tilted around $Ox_3 = Ox_3^{'}$ by an angle θ from Ox_1x_3. The methodology consists in representing the crack by a continuous distribution of three families *j* (*j*= 1, 2 and 3) of elliptical dislocations the Burgers vectors of which $\vec{b}_j$ are linked to the crack and directed along $x_j^{'}$. The displacement and stress fields of the dislocations are first given. The equilibrium distribution functions D_j of the dislocations *j* satisfy, separately, to a singular integral equation whose form closer to the crack-tip is the simple Cauchy type; this allows to express D_j and corresponding relative displacement ϕ_j of the faces of the crack about the crack-tip, crack-tip stresses, and the average crack extension force $<G>$ (per unit length of the crack front), averaged over the length of the crack-front. For relatively low values of $M_{12} = \sigma_{21}^{a} / \sigma_{22}^{a}$ ($|M_{12}| \leq 6$), $< G >$ as a function of θ exhibits positive maxima in tension $\sigma_{22}^{a} > 0$ for $\theta_{max} \cong 53°$ and in compression $\sigma_{22}^{a} < 0$ for $\theta_{max} \cong 42°$. θ_{max} decreases (resp. increases) with increasing M_{12} in tension (resp. compression). σ_{22}^{a} provides positive contributions to < G > indicating that the expansion of the elliptic crack in its own plane is feasible in tension. The shears σ^a_{21} and σ^a_{23} when parallel to the plane of the loop contribute negative values to < G > suggesting that an elliptical crack is unable to expand in its own plane under a shearing stress that lies in its plane. Under such conditions, the planar elliptic crack is not the right configuration to dealt with crack nucleation in brittle solids under applied mixed mode *I+II+III* loading. We would have to start, from the beginning of crack expansion analysis, with a non-planar crack loop whose front should be locally of arbitrary shape.

Keywords : *fracture mechanics, linear elasticity, crack propagation and arrest, dislocations, crack extension force.*

RÉSUMÉ

Fissure elliptique sous sollicitations extérieures arbitraires : dislocation, contrainte en tête de fissure et force d'extension de fissure

Une fissure elliptique de centre O, dans un milieu élastique isotrope infiniment étendu et sollicité uniformément de manière arbitraire à l'infini, fait l'objet de la présente étude. La tension appliquée σ^a_{22} agit dans la direction verticale x_2 et les cisaillements σ^a_{21} et σ^a_{23} agissent dans les directions x_1 et x_3, respectivement. Les contraintes normales de Poisson $-\nu\sigma^a_{22}$ (ν est le rapport de Poisson) agissant dans les directions x_1 et x_3 sont intégrées à l'analyse. La fissure est dans le plan (π) = $Ox'_1x'_3$ inclinée autour de Ox_3= Ox'_3 d'un angle θ à partir de Ox_1x_3. La méthodologie consiste à représenter la fissure par une distribution continue de trois familles j (j = 1, 2 et 3) de dislocations elliptiques dont les vecteurs de Burgers $\vec{b}_j$ sont liés à la fissure et orientés selon x'_j. Les champs élastiques des dislocations sont d'abord donnés. Les fonctions de distribution d'équilibre D_j des dislocations j satisfont séparément à une équation intégrale singulière dont la forme plus proche du fond de fissure est du type simple de Cauchy ; cela permet d'exprimer D_j au niveau du front de fissure ainsi que le déplacement relatif correspondant ϕ_j des faces de la fissure. Les contraintes au niveau du front de fissure sont ensuite déduites de superpositions de contraintes de dislocations individuelles, en plus de la force d'extension de fissure moyenne < G > (par unité de longueur du front de fissure), moyennée sur la longueur du front de fissure. Pour des valeurs relativement faibles de $M_{12} = \sigma^a_{21} / \sigma^a_{22}$ ($|M_{12}| \leq 6$), < G > en fonction de θ exhibe des maximums positifs en tension σ^a_{22} > 0 pour $\theta_{max} \cong 53$ ° et en compression σ^a_{22} < 0 pour

$\theta_{max} \cong 42$. θ_{max} décroit (resp. croit) lorsque M_{12} croit en tension (resp. compression). La contrainte σ_{22}^{a} fournit des contributions positives à $< G >$ indiquant que l'expansion de la fissure elliptique dans son propre plan est réalisable en traction. Les cisaillements σ_{21}^{a} et σ_{23}^{a} lorsqu'ils sont parallèles à la boucle contribuent par des valeurs négatives à $< G >$ suggérant qu'une fissure elliptique est incapable de se dilater dans son propre plan sous une contrainte de cisaillement qui se trouve dans son plan. Dans de telles conditions, la fissure elliptique plane n'est pas la bonne configuration pour traiter la nucléation/initiation de fissure dans les solides fragiles sollicités en mode mixte *I+II+III*.

Mots-clés : *mécanique de la rupture, élasticité linéaire, propagation et arrêt de fissure, dislocation, force d'extension de fissure.*

I - INTRODUCTION

In the stage of nucleation / initiation of a crack in a homogeneous elastic material under load, consider a crack in the form of a closed loop. A question that arises is under what condition the crack will develop. The answer is that the crack should expand in the configuration which corresponds to a maximum decrease in the energy of the system (elastic energy + potential energy of the loading mechanism). The most general approach is to start the analysis with a non-plane loop whose front is locally of arbitrary shape, calculate the extension force G of the crack (per unit length of the crack front), take the mean value $< G >$ of G averaged over all the crack front and seek under which crack-front configuration $< G >$ is maximum. It is in this configuration that the crack will expand under arbitrary general stresses as soon as

$$< G >_{max} = 2\,\gamma. \tag{1}$$

Here γ is the surface energy. Concretely, it is in a later stage corresponding to the propagation of the crack over large distances that this general approach was carried out. Locally, the crack front can be considered plane, perpendicular to the direction of fracture propagation, and the arbitrary shape of the crack can be developed in the form of Fourier series [1 - 5]. Coming back to finite crack loops, this is the elliptic crack that is well documented, either under tension or shears or both ([6 - 9] to quote earliest works only). A common procedure is to look for defect elastic fields that satisfy the equations of equilibrium coupled with boundary conditions (at the defect surface for instance) [6 - 8]. Eshelby's way [9] saves the use of ellipsoidal co-ordinates and the search for suitable stress functions or match stress and displacement at an interface. These elastic fields thus obtained can be used to study the expansion of an elliptical crack in its plane while keeping in mind that this expansion may not correspond to that observed as underlined above: this is the difficulty encountered in fracture mechanics when the starter crack has an imposed shape. The objective of the present study is to investigate the expansion of an elliptical crack in its own plane under arbitrary applied loadings by representing the crack by a continuous distribution of elliptical dislocations. ***Figure 1*** serves to illustrate the modelling.

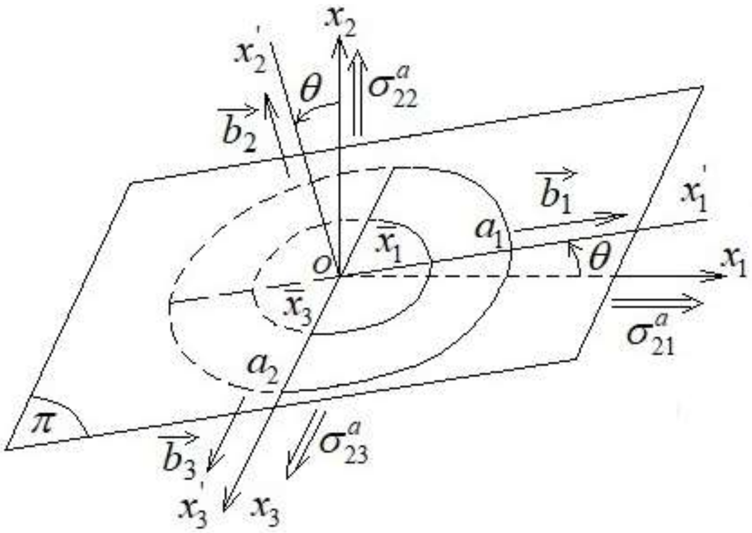

Figure 1 : *Elliptical crack of centre O and semiaxes a_1 and a_2 along x_1' and x_3'. The applied tension σ_{22}^a acts in the vertical x_2 - direction and the shears σ_{21}^a and σ_{23}^a (parallel to the horizontal x_1x_3- plane) act in the x_1 and x_3 directions. The crack is in the plane $(\pi)= Ox_1'x_3'$ tilted around $Ox_3 = Ox_3'$ by an angle θ from Ox_1x_3. The portions of the ellipse above and below the horizontal plane are solid and dashed as also are an elliptical crack dislocation with semiaxes $x_1' = \bar{x}_1$ and $x_3' = \bar{x}_3$. The Burgers vectors $\vec{b}_j$ of the crack dislocations (j) are directed along x_j'*

We consider an infinitely extended isotropic elastic medium containing in its interior an elliptical crack with centre *O*, with semiaxes a_1 and a_2 along x_1' and x_3'. The crack is in the $(\pi)= Ox_1'x_3'$ plane. It is made up of three families *j* (*j* = 1, 2 and 3) of elliptical dislocations with Burgers vectors $\vec{b}_j$ along x_j'. The medium is stressed uniformly at infinity with a tension σ_{22}^a in the vertical x_2 -direction and shears σ_{21}^a and σ_{23}^a (parallel to the horizontal x_1x_3- plane) in the x_1 and x_3 directions. The plane *(π)* = $Ox_1^{'}x_3^{'}$ is inclined around the x_3 - direction by the angle θ from Ox_1x_3. The equation of the ellipse is given by :

$$\left(\frac{x_1^{'}}{a_1}\right)^2 + \left(\frac{x_3^{'}}{a_2}\right)^2 = 1 . \tag{2}$$

Distribution functions D_j of the dislocations j are defined such that $D_j(\bar{x}_1)d\bar{x}_1$ represents the number of dislocations j in a small interval $d\bar{x}_1$ located at the position $x_1^{'} = \bar{x}_1$ on the $Ox_1^{'}$ - axis. To that position of the dislocations correspond the position $x_3^{'} = \bar{x}_3$ on the $Ox_3^{'}$ - axis. The following proportionality relation is assumed :

$$a_1\bar{x}_3 = a_2\bar{x}_1 \ . \tag{3}$$

(3) is used in the calculation of the crack extension force G (per unit length of the crack front) as explained below (Section 2). Hence, we admit that $D_j(\bar{x}_1) = D_j(\bar{x}_3)$; this conforms with the result that the relative displacement of the faces of the crack ϕ_j is an ellipse (see [7] and [9], for example). The elastic fields in the fractured medium read as a superposition of the elastic fields of the crack dislocations. When the dislocations are circular, stress fields of families 1 and 3 (glide dislocations) have been obtained by Keller as recorded by Kröner [10] and those for dislocation 2 (prismatic loop) by Kroupa [11]. By line integration of the Peach-Koehler equation for a circular dislocation loop, recent stress expressions for these dislocations have been presented [12]. Representations of elastic fields of circular dislocations in terms of spherical harmonics are displayed by [13]. Elastic fields of elliptical dislocations are uncommonly reported. We shall provide expressions for these using the method called “Method of Fourier series or integrals” in review works by Mura [14, 15]: the method consists in writing the plastic distortions associated with the dislocation in Fourier integral series forms. The displacement associated with a single wave (*i.e.* simple sinusoidal) plastic distortion is available from [14, 15]. Those of the dislocation are derived by superposition. In Section 2 (Methodology), the procedures for determining the elastic fields of the dislocations and crack analysis are explained. In Section 3, are given the elastic fields (stress and displacement) of the elliptical dislocations j, distribution functions D_j of the crack dislocations and corresponding relative displacement ϕ_j of the faces of the crack, crack-tip stress and crack extension force G per unit length of the crack front, assuming the crack to expand in its own plane. Sections 4 and 5 are devoted to discussion of the results and conclusion, respectively.

II - METHODOLOGY

II-1. Elastic fields of elliptical crack dislocations

The three types *j* (*j*=1, 2 and 3) of crack dislocation considered have Burgers vectors $\vec{b}_1 = (b, 0, 0)$, $\vec{b}_2 = (0, b, 0)$ and $\vec{b}_3 = (0, 0, b)$ along $x_j^{'}$; they spread in the $Ox_1^{'}x_3^{'}$-plane in the form (2). We shall make use of the displacement $u_m(\vec{x}^{'})$, *m*=1, 2 and 3, (see (5) below) due to a plastic distortion $\beta_{ij}^{*}(\vec{x}^{'})$ given as a periodic function of coordinates $\vec{x}^{'} = (x_1^{'}, x_2^{'}, x_3^{'})$

$$\beta_{ij}^{*} = \overline{\beta}_{ij}^{*}(\vec{k}^{'})e^{i\vec{k}^{'}.\vec{x}^{'}} \quad (4)$$

where $\vec{k}^{'} = (k_1^{'}, k_2^{'}, k_3^{'})$ with $k_j^{'}$ arbitrary constants. Mura [14, 15] has shown the associated displacement component to be

$$\overline{u}_m(\vec{x}^{'}) = -ik_l^{'}C_{klji}L_{mk}\overline{\beta}_{ij}^{*}e^{i\vec{k}^{'}.\vec{x}^{'}}. \quad (5)$$

For isotropic material,

$$L_{mk} = \frac{\delta_{km}(\lambda + 2\mu)k^{'2} - k_k^{'}k_m^{'}(\lambda + \mu)}{\mu(\lambda + 2\mu)k^{'4}} \quad (6)$$

where $k^{'2} = k_1^{'2} + k_2^{'2} + k_3^{'2}$ and

$$C_{klji} = \lambda\delta_{kl}\delta_{ji} + \mu\delta_{kj}\delta_{li} + \mu\delta_{ki}\delta_{lj}, \quad (7)$$

δ_{ij} being the Kronecker delta and λ and μ are Lamé's constants. The plastic distortions $\beta_{ij}^{*(l)}$ associated to the dislocations *l* (*l*= 1, 2 and 3), are expressed successively.

$$\beta_{21}^{*(1)} = b\delta(x_2^{'})\left(H\left[x_1^{'} + a_1\sqrt{1 - x_3^{'2}/a_2^2}\right] - H\left[x_1^{'} - a_1\sqrt{1 - x_3^{'2}/a_2^2}\right]\right), \quad \left|x_3^{'}\right| \leq a_2$$

$$= \frac{ba_1a_2}{(2\pi)^2}\int_{-\infty}^{\infty}\int_{-\infty}^{\infty}\int_{-\infty}^{\infty}\frac{J_1[\eta_2]}{\eta_2}e^{i\vec{k}^{'}.\vec{x}^{'}}d\vec{k}^{'}; \quad (8)$$

$J_1[\eta_2]$ is the Bessel function of the first kind; $\beta_{21}^{*(1)} = 0$ for $\left|x_3^{'}\right| \geq a_2$, $\eta_2^2 = a_1^2k_1^{'2} + a_2^2k_3^{'2}$, $d\vec{k}^{'} = dk_1^{'}dk_2^{'}dk_3^{'}$ and, δ and H are the Dirac delta and

Heaviside step functions, respectively. The other components of the plastic distortion are zero. $\beta_{21}^{*(1)}$ in its Fourier form is a superposition of expressions of the form (4). Therefore, associated displacements $u_m^{(1)}$ (m=1, 2 and 3) are similar superpositions of the displacement (5). Making use of (6) and (7), we write

$$u_m^{(1)} = -i\frac{ba_1a_2}{(2\pi)^2}\int_{-\infty}^{\infty}\int_{-\infty}^{\infty}\int_{-\infty}^{\infty}\frac{1}{k'^2}\left(k_2'\delta_{m1} + k_1'\delta_{m2} - \frac{k_1'k_2'}{(1-\nu)k'^2}\right.$$
$$\left.\times\left[k_1'\delta_{m1} + k_2'\delta_{m2} + k_3'\delta_{m3}\right]\right)\frac{J_1[\eta_2]}{\eta_2}e^{i\vec{k}'.\vec{x}'}d\vec{k}' . \qquad (9)$$

Performing the necessary integrations in (9) provide the displacements in Cartesian coordinates. We now consider the dislocation j= 2 with form (2) and Burgers vector $\vec{b}_2 = (0, b, 0)$ along x_2'. There are only two non-zero components $\beta_{12}^{*(2)}$ and $\beta_{32}^{*(2)}$ of the plastic distortion.

$$\beta_{12}^{*(2)} = bH(x_2')\left(\delta\left[x_1' + a_1\sqrt{1 - x_3'^2/a_2^2}\right] - \delta\left[x_1' - a_1\sqrt{1 - x_3'^2/a_2^2}\right]\right)$$
$$= \frac{ba_1a_2}{(2\pi)^2}\int_{-\infty}^{\infty}\int_{-\infty}^{\infty}\int_{-\infty}^{\infty}\frac{k_1'}{k_2'}\frac{J_1[\eta_2]}{\eta_2}e^{i\vec{k}'.\vec{x}'}d\vec{k}' \ ;$$
$$\beta_{32}^{*(2)} = bH(x_2')\left(\delta\left[x_3' + a_2\sqrt{1 - x_1'^2/a_1^2}\right] - \delta\left[x_3' - a_2\sqrt{1 - x_1'^2/a_1^2}\right]\right)$$
$$= \frac{ba_1a_2}{(2\pi)^2}\int_{-\infty}^{\infty}\int_{-\infty}^{\infty}\int_{-\infty}^{\infty}\frac{k_3'}{k_2'}\frac{J_1[\eta_2]}{\eta_2}e^{i\vec{k}'.\vec{x}'}d\vec{k}' \ . \qquad (10)$$

Making use of (5) and (6), we obtain

$$u_m^{(2)} = -i\frac{ba_1a_2}{(2\pi)^2}\int_{-\infty}^{\infty}\int_{-\infty}^{\infty}\int_{-\infty}^{\infty}\frac{k_1'\delta_{m1} + k_3'\delta_{m3}}{1-\nu}$$
$$\times\left(-\frac{\nu}{k'^2} + \frac{k_2'^2}{k'^4}\right)\frac{J_1[\eta_2]}{\eta_2}e^{i\vec{k}'.\vec{x}'}d\vec{k}' \ , \qquad m= 1 \text{ and } 3$$
$$u_2^{(2)} = -i\frac{ba_1a_2}{(2\pi)^2}\int_{-\infty}^{\infty}\int_{-\infty}^{\infty}\int_{-\infty}^{\infty}\left(\frac{1}{k_2'} - \frac{(2-\nu)k_2'}{(1-\nu)k'^2}\right.$$
$$\left. + \frac{k_2'^3}{(1-\nu)k'^4}\right)\frac{J_1[\eta_2]}{\eta_2}e^{i\vec{k}'.\vec{x}'}d\vec{k}' . \qquad (11)$$

We consider the dislocation j = 3 with form (2) and Burgers vector $\vec{b}_3 = (0,0,b)$ along $x_3^{'}$. For the plastic distortion, we have

$$\beta_{23}^{*(3)} = b\delta(x_2^{'})H\left(\left[x_1^{'} + a_1\sqrt{1-x_3^{'2}/a_2^2}\right]\left[a_1\sqrt{1-x_3^{'2}/a_2^2} - x_1^{'}\right]\right), \quad \left|x_3^{'}\right| \le a_2$$

$$= \frac{ba_1a_2}{(2\pi)^2}\int_{-\infty}^{\infty}\int_{-\infty}^{\infty}\int_{-\infty}^{\infty}\frac{J_1[\eta_2]}{\eta_2}e^{i\vec{k}^{'}.\vec{x}^{'}}d\vec{k}^{'} \;; \tag{12}$$

$\beta_{23}^{*(3)} = 0$ for $\left|x_3^{'}\right| \ge a_2$ and the other components of the plastic distortion are zero. (12) and (8) are identical although their Cartesian form is written differently. Making use of (5) to (7), we obtain (m= 1, 2 and 3)

$$u_m^{(3)} = -i\frac{ba_1a_2}{(2\pi)^2}\int_{-\infty}^{\infty}\int_{-\infty}^{\infty}\int_{-\infty}^{\infty}\frac{1}{k^{'2}}\left(k_3^{'}\delta_{m2} + k_2^{'}\delta_{m3} - \frac{k_2^{'}k_3^{'}}{(1-\nu)k^{'2}}\right.$$
$$\left.\times\left[k_1^{'}\delta_{m1} + k_2^{'}\delta_{m2} + k_3^{'}\delta_{m3}\right]\right)\frac{J_1[\eta_2]}{\eta_2}e^{i\vec{k}^{'}.\vec{x}^{'}}d\vec{k}^{'}. \tag{13}$$

At this stage, we can write down the various displacements $\vec{u}^{(j)}$ (j= 1, 2 and 3) associated with the three types j of crack dislocation with form (2). The stress fields $(\sigma)^{(j)}$ can be obtained by differentiating the displacements. Our calculation results are displayed in Section 3.

II-2. Crack analysis

The crack system ***(Figure 1)*** has been described earlier in Section 1. The condition that the crack faces remain free from any traction is adopted; this gives

$$\begin{aligned}\bar{\sigma}_{12} &= 0\\ \bar{\sigma}_{22} &= 0\,.\\ \bar{\sigma}_{23} &= 0\end{aligned} \tag{14}$$

$\bar{\sigma}_{ij}(\vec{x}^{'})$ stands for the total stress at any point $\vec{x}^{'} = (x_1^{'}, x_2^{'}, x_3^{'})$ in the medium and is linked to D_j. In (14), we are concerned with the positions on the crack faces only. We write $\bar{\sigma}_{ij}$ as

$$\bar{\sigma}_{ij} = \sigma_{ij}^{A} + \sigma_{ij}^{(C)(1)} + \sigma_{ij}^{(C)(2)} + \sigma_{ij}^{(C)(3)} \quad . \tag{15}$$

$(\sigma)^A$ is the externally applied stress including normal induced stresses from Poisson effect; relatively to $x_i^{'}$, its components are

$$\sigma_{11}^A = \left[-\nu_A + (1+\nu_A)\sin^2\theta\right]\sigma_{22}^a + \sin 2\theta\,\sigma_{21}^a$$
$$\sigma_{21}^A = (1+\nu_A)\sin 2\theta\sigma_{22}^a / 2 + \cos 2\theta\,\sigma_{21}^a$$
$$\sigma_{13}^A = \sin\theta\,\sigma_{23}^a$$
$$\sigma_{22}^A = \left[1-(1+\nu_A)\sin^2\theta\right]\sigma_{22}^a - \sin 2\theta\,\sigma_{21}^a$$
$$\sigma_{23}^A = \cos\theta\,\sigma_{23}^a$$

$$\sigma_{33}^A = -\nu_A\sigma_{22}^a\,. \tag{16}$$

ν_A is Poisson's ratio ν so denoted to track the contributions of the Poisson's stress.

$$\sigma_{ij}^{(C)(m)}(\vec{x}^{'}) = \int_0^{a_1}\sigma_{ij}^{(m)}\left(\vec{x}^{'};\overline{x}_1\right)D_m(\overline{x}_1)d\overline{x}_1 \quad (m=1,\,2 \text{ and } 3) \tag{17}$$

$\sigma_{ij}^{(m)}$ is the stress field at $\vec{x}^{'} = (x_1^{'}, x_2^{'}, x_3^{'})$ due to the elliptical crack dislocation m with position $x_1^{'} = \overline{x}_1$ along $x_1^{'}$ in the distribution ***(Figure 1)***. (14) gives three integral equations the resolution of which yields the D_m. The relative displacements ϕ_m of the faces of the crack in the $x_m^{'}$-direction (m= 1, 2 and 3) are obtained by integration from the relation $d\phi_m = -bD_m(x_1^{'})dx_1^{'}$:

$$\phi_m = \int_{x_1^{'}}^{a_1} bD_m(x_1)dx_1\,,\ \left|x_1^{'}\right| \le a_1\,. \tag{18}$$

From (21) to (23), one can obtain the crack-tip stresses. The crack extension force G per unit length of the crack front is defined in previous works (see [16, 3], for example). We shall refer to ***Figure 2*** as illustration to write down an expression for G under the requirement that the crack loop expands in its own plane. Allow the elliptical crack with semiaxes a_1 and a_2 on the $x_1^{'}$ and $x_3^{'}$ axes to advance steady from a_1 to $a_1+\delta a_1$ and a_2 to $a_2 + \delta a_2$ but apply forces to the freshly formed surfaces to prevent relative displacements; the energy of the system is unaltered. Now allow these forces to relax to zero so that the crack extends effectively from a_1 to $a_1+\delta a_1$ and a_2 to $a_2 + \delta a_2$ on the $x_1^{'}$ and $x_3^{'}$ axes.

The work done by these forces corresponds to a decrease of the energy of the system that we shall estimate (the energy of the system consists of the elastic energy plus the potential energy of the loading mechanism). We take a position P on the freshly formed surface ***(Figure 2)*** to which we attach a surface element $ds = \left| d\rho \vec{e}_\rho \wedge \overrightarrow{PP'} \right|$ with $\vec{e}_\rho = \overrightarrow{OP} / OP$. The energy change associated with ds is $(ds \sum_i \bar{\sigma}_{i2} \Delta u^{(i)} / 2)$ where $\Delta u^{(i)}$ is the difference in displacement across the lengthened crack just behind its tip, in the $x_i^{'}$ - direction. When the crack advances from $x_1^{'} = a_1$ to $a_1 + \delta a_1$ and $x_3^{'} = a_2$ to $a_2 + \delta a_2$ on the $x_1^{'}$ and $x_3^{'}$ axes, the energy decrease ($-\delta E$) associated with a surface element

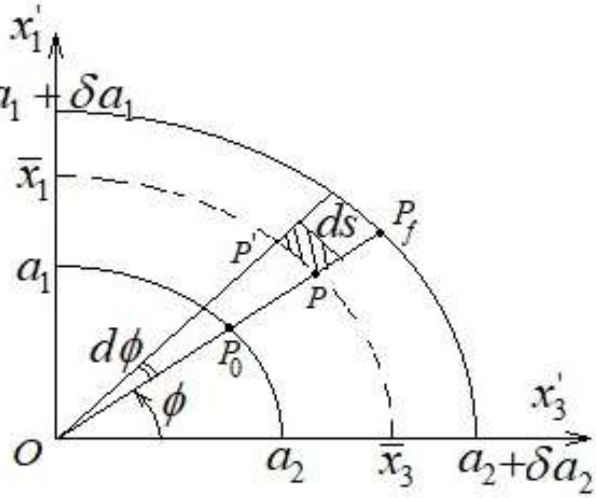

Figure 2 : *To illustrate the calculation of the crack extension force G. Elliptical crack front allowed to advance steadily from* a_1 *to* $a_1+\delta a_1$ *and* a_2 *to* $a_2 + \delta a_2$ *along* $x_1^{'}$ *and* $x_3^{'}$ *axes. An arbitrary point P (* $x_1^{'} = \rho \sin\phi$, $x_3^{'} = \rho\cos\phi$ *) on the newly created surface is indicated to which is associated a surface element ds (hatched). At fixed* ϕ*, as the crack expands, P moves from* P_0 *(* $x_1^{'} = \rho_0 \sin\phi$, $x_3^{'} = \rho_0 \cos\phi$ *) on the shorter crack to* P_f *(* $x_1^{'} = \rho_f \sin\phi$, $x_3^{'} = \rho_f \cos\phi$ *) on the lengthened crack front. P' is the position of P on an elliptical crack dislocation after a change* $d\phi$ *of the polar angle* ϕ*; the crack dislocation meets the* $x_1^{'}$ *and* $x_3^{'}$ *axes at* $\bar{x}_1$ *and* $\bar{x}_3$ *such that* $a_2\bar{x}_1 = a_1\bar{x}_3$

$$\Delta s = \int_{\rho_0}^{\rho_f} ds \cong \rho_0^2 \left(\sin^2\phi + a_r^2 \cos^2\phi\right) d\phi \delta a_1 / a_1 \tag{19}$$

($a_r = a_1 / a_2$ and δa_1 being small and, when used below, will be let to go to zero.) is given as

$$-\delta E = \frac{1}{2}\int_{\rho_0}^{\rho_f}\sum_{i=1}^{3}\bar{\sigma}_{i2}\Delta u^{(i)}\rho\left(\sin^2\phi + a_r^2\cos^2\phi\right)d\rho d\phi\,, \tag{20}$$

the integration being performed with respect to ρ only. The crack extension force G (per unit length of the crack front) at P_0 is defined as

$$G = \lim_{\delta a_1 \to 0} -\delta E / \Delta s\,. \tag{21}$$

Expressions for G are given in Section 3.

III - RESULTS

III-1. Elastic fields of crack dislocations

For $x_2^{'} \neq 0$, the displacements due to the dislocations j (j=1, 2 and 3) read :

$$u_m^{(1)} = \frac{ba_1a_2}{8\pi(1-\nu)}\left\| -2(1-\nu)\delta_{m1}\frac{\partial}{\partial x_2^{'}} - (1-2\nu)\delta_{m2}\frac{\partial}{\partial x_1^{'}} + x_2^{'}\left(\delta_{m1}\frac{\partial^2}{\partial x_1^{'2}} + \delta_{m2}\frac{\partial^2}{\partial x_2^{'}\partial x_1^{'}} + \delta_{m3}\frac{\partial^2}{\partial x_3^{'}\partial x_1^{'}}\right)\right\| A^*\,,$$

$$u_m^{(2)} = -\frac{ba_1a_2}{8\pi(1-\nu)}\left(\delta_{m2}4(1-\nu)H(x_2^{'})\frac{\partial}{\partial x_2^{'}}A^*(x_2^{'}=0) + \left\|(1-2\nu)\left[\delta_{m1}\frac{\partial}{\partial x_1^{'}} + \delta_{m3}\frac{\partial}{\partial x_3^{'}}\right] + \delta_{m2}2(1-\nu)\frac{\partial}{\partial x_2^{'}} + x_2^{'}\left[\delta_{m1}\frac{\partial^2}{\partial x_2^{'}\partial x_1^{'}} - \delta_{m2}\frac{\partial^2}{\partial x_2^{'2}} + \delta_{m3}\frac{\partial^2}{\partial x_2^{'}\partial x_3^{'}}\right]\right\| A^*\right),$$

$$u_m^{(3)} = \frac{ba_1a_2}{8\pi(1-\nu)}\left\| -\delta_{m2}(1-2\nu)\frac{\partial}{\partial x_3^{'}} - \delta_{m3}2(1-\nu)\frac{\partial}{\partial x_2^{'}} + x_2^{'}\left(\delta_{m1}\frac{\partial^2}{\partial x_1^{'}\partial x_3^{'}} + \delta_{m2}\frac{\partial^2}{\partial x_2^{'}\partial x_3^{'}} + \delta_{m3}\frac{\partial^2}{\partial x_3^{'2}}\right)\right\| A^*;\ m = 1, 2 \text{ and } 3 \tag{22}$$

$$A^* = \int_{-\infty}^{\infty}\int_{-\infty}^{\infty} \frac{e^{-x_2'\eta_1}}{\eta_1}\frac{J_1[\eta_2]}{\eta_2} e^{i(k_1'x_1'+k_3'x_3')} dk_1' dk_3', \quad (23)$$

$\eta_1^2 = k_1'^2 + k_3'^2$. In use we take

$$A^* = -\frac{2\pi x_2'}{a_1 a_2} - 4\int_0^{\pi/2} \frac{\bar{A}^*}{a^{*2}} d\psi\,; \quad (24)$$

$$\bar{A}^* = \int_{x_2'}^{\infty} r\left(1 + \frac{\Omega^2}{r^2}\left[\frac{a^{*2}}{\left(1-r^2\right)^2} + \frac{x^2}{r^4}\right]^{-1}\right) dx, \qquad a^{*2} = a_2^2\left(1 - \left[1 - a_r^2\right]\sin^2\psi\right),$$

$$\Omega = \sin\psi\, x_1' + \cos\psi\, x_3', \qquad \frac{1}{r^2} = \frac{2\Omega^2}{\Omega^2 - a^{*2} - x^2 + \sqrt{\bar{\Delta}}},$$

$$\bar{\Delta} = \left(a^{*2} + x^2 - \Omega^2\right)^2 + 4\Omega^2 x^2 .$$

The stress fields are obtained by differentiating the displacements. For $x_2' = 0$, it is safer to put $x_2' = 0$ in the Fourier forms of the elastic fields (such as (9), (11) and (13), for example) before integrating with respect to k_i'. We display below stresses used in the crack analysis. For $x_2' = 0$:

$$\sigma_{12}^{(1)} = -C_1 a_1 a_2 \int_{-\pi/2}^{\pi/2} \left[1 - \nu\cos^2\psi\right] M^* d\psi$$

$$\sigma_{23}^{(1)} = -\frac{1}{2}\nu C_1 a_1 a_2 \int_{-\pi/2}^{\pi/2} \sin 2\psi M^* d\psi = \sigma_{12}^{(3)}$$

$$\sigma_{22}^{(1)} = 0 = \sigma_{22}^{(3)}$$

$$\sigma_{23}^{(3)} = -C_1 a_1 a_2 \int_{-\pi/2}^{\pi/2} \left[1 - \nu + \nu\cos^2\psi\right] M^* d\psi$$

$$\sigma_{22}^{(2)} = C_1 a_1 a_2 \int_{-\pi/2}^{\pi/2} M^* d\psi$$

$$\sigma_{12}^{(2)} = 0 = \sigma_{23}^{(2)} \quad (25)$$

where $C_1 = \mu b / 2\pi(1-\nu)$ and

$$M^* = \begin{cases} (a^{*2} - \Omega^2)^{-3/2} & \text{for } \Omega^2 / a^{*2} < 1 \\ \infty & \Omega^2 / a^{*2} = 1 \\ 0 & \Omega^2 / a^{*2} > 1 \end{cases} . \quad (26)$$

III-2. Crack dislocation distributions

We use the condition (14) for traction-free at the crack faces and associated stress quantities (16), (17) and (25) at positions $P_C(x_1^{'}, x_2^{'}=0, x_3^{'}=0)$, $\left|x_1^{'}\right| < a_1$, to obtain the following integral equations for the D_j:

$$\sigma_{12}^{A} + 2C_1 a_r^2 \int_{x_1^{'}}^{a_1} d\bar{x}_1 D_1(\bar{x}_1)\frac{1}{\bar{x}_1}\left(\frac{\nu F(\pi/2,\bar{y}_1)}{\bar{y}_1^2} + \left[\nu - 1 - \nu/\bar{y}_1^2\right]\Pi(\pi/2,\bar{y}_1^2,\bar{y}_1)\right) = 0$$

$$\sigma_{22}^{A} + 2C_1 a_r^2 \int_{x_1^{'}}^{a_1} d\bar{x}_1 D_2(\bar{x}_1)\frac{1}{\bar{x}_1}\Pi(\pi/2,\bar{y}_1^2,\bar{y}_1) = 0$$

$$\sigma_{23}^{A} - 2C_1 a_r^2 \int_{x_1^{'}}^{a_1} d\bar{x}_1 D_3(\bar{x}_1)\frac{1}{\bar{x}_1}\left(\frac{\nu F(\pi/2,\bar{y}_1)}{\bar{y}_1^2} + \left[1 - \nu/\bar{y}_1^2\right]\Pi(\pi/2,\bar{y}_1^2,\bar{y}_1)\right) = 0 \quad ;$$

(27)

$$F(\pi/2,\bar{y}_1) = \int_0^{\pi/2} \frac{d\psi}{\sqrt{1-\bar{y}_1^2\sin^2\psi}},$$

$$\Pi(\pi/2,\bar{y}_1^2,\bar{y}_1) = \int_0^{\pi/2} \frac{d\psi}{(1-\bar{y}_1^2\sin^2\psi)\sqrt{1-\bar{y}_1^2\sin^2\psi}}$$

are complete elliptic integral of first and third kind, respectively; $\bar{y}_1^2 = a_r^2 x_1^{'2}/\bar{x}_1^2 + 1 - a_r^2$. As P_C moves closer to the crack-tip, (*i.e.* $x_1^{'} \to a_1$), (27) becomes

$$\sigma_{12}^{A} - C_1 \int_{1-\delta\bar{y}_1}^{1} d\bar{y}_1 D_1(\bar{y}_1)\frac{1}{1-\bar{y}_1} = 0$$

$$\sigma_{22}^{A} + C_1 \int_{1-\delta\bar{y}_1}^{1} d\bar{y}_1 D_2(\bar{y}_1)\frac{1}{1-\bar{y}_1} = 0$$

$$\sigma_{23}^{A} - (1-\nu)C_1 \int_{1-\delta\bar{y}_1}^{1} d\bar{y}_1 D_3(\bar{y}_1)\frac{1}{1-\bar{y}_1} = 0; \qquad (28)$$

$0 < \delta\bar{y}_1 \ll 1$, $\delta\bar{y}_1$ is a finite sufficiently small real, a fraction of unity. Using Muskhelishvili [17] (his relations (88.8 to 88.11), p. 251), we arrive at

$$D_j \cong \alpha_0 \alpha_j \frac{1}{\sqrt{1-y_1^{'}}} \quad ; \qquad (j=1,\ 2 \text{ and } 3) \qquad (29)$$

$$y_1^{'2} = a_r^2 x_1^{'2} / a_1^2 + 1 - a_r^2,$$
$$\alpha_j = \frac{1}{\pi C_1}\left(-\sigma_{12}^A \delta_{j1} + \sigma_{22}^A \delta_{j2} - \delta_{j3}\sigma_{23}^A / (1-\nu)\right),$$
$$\alpha_0 = \sqrt{\delta y_1^{'}}$$

$\delta y_1^{'}$ is of the order (or a fraction) of unity. (29) is the value of the dislocation j distribution closer to the crack tip. The associated relative displacement of the faces of the crack is (under the condition $a_r^2 \leq 1$)

$$\phi_j \cong 2b\alpha_0\alpha_j a_2 \left(-\frac{\sqrt{1-a_r^2}}{\sqrt{1+\sqrt{1-a_r^2}}} F(\lambda, \overline{p}) + \sqrt{1+\sqrt{1-a_r^2}}\, E(\lambda, \overline{p}) \right); \qquad (30)$$
$$\lambda = \frac{\sqrt{1-y_1^{'}}}{\sqrt{1-\sqrt{1-a_r^2}}}, \quad \overline{p} = \frac{\sqrt{1-\sqrt{1-a_r^2}}}{\sqrt{1+\sqrt{1-a_r^2}}}$$

F and E are the elliptic integral of the first and second kind, respectively. (30) is given for $a_r^2 \leq 1$ but this restriction disappears in the expression for G that follows.

III-3. Crack-tip Stress and crack extension force

To obtain the crack extension force G (section 2), it is required to express the crack-tip $\overline{\sigma}_{ij}$ stresses at P ***(Figure 2)*** ahead of the shorter crack or equivalently as performed below behind the lengthened crack. The crack-tip stresses may be identified to the following expression

$$\overline{\sigma}_{ij}(P) = \sum_{m=1}^{3} \int_{a_1}^{a_1+\delta a_1} \sigma_{ij}^{(m)}(P; \overline{x}_1^{'}) D_m(\overline{x}_1^{'}) d\overline{x}_1^{'}, \qquad \delta a_1 << a_1$$
$$= \sum_{m=1}^{3} \int_{\overline{x}_1}^{a_1+\delta a_1} \sigma_{ij}^{(m)}(P; \overline{x}_1^{'}) D_m(\overline{x}_1^{'}) d\overline{x}_1^{'} \equiv \sum_{m=1}^{3} \overline{\sigma}_{ij}^{(m)}. \qquad (31)$$

The lower limit of integration goes from a_1 to $\overline{x}_1$ because, from the stress expressions (25), the elliptical crack dislocations passing through positions between P_0 and P ***(Figure 2)*** contribute nothing. The relation (3) applies to any crack dislocation. (29) is used for $D_m(\overline{x}_1^{'})$ where for the lengthened crack

$y_1'^2 = a_r^2 \bar{x}_1'^2 / (a_1 + \delta a_1)^2 + 1 - a_r^2$; this applies also to ϕ_m (30) that will be used for $\Delta u^{(m)}$ (20) in the calculation of G (21). We may write in contracted form

$$\delta_{m1}\bar{\sigma}_{12} + \delta_{m2}\bar{\sigma}_{22} + \delta_{m3}\bar{\sigma}_{23} = -2C_1\alpha_0 a_r \sqrt{\frac{\delta a_1}{a_1}} \left(\int_{-\pi/2}^{0} + \int_{0}^{\pi/2} \right) \frac{d\psi}{\bar{a}^{*3}\left(1-b^{*2}\right)^{3/2}}$$
$$\times\Big(\delta_{m1}\left[\alpha_1(1-\nu\cos^2\psi) + \alpha_3\nu\sin 2\psi/2\right] - \delta_{m2}\alpha_2$$
$$+\delta_{m3}\left[\alpha_3(1-\nu+\nu\cos^2\psi) + \alpha_1\nu\sin 2\psi/2\right]\Big), \quad m=1,2 \text{ and } 3 \qquad (32)$$

where $\bar{a}^{*2} = a_r^{-2}\left(1-\left[1-a_r^2\right]\sin^2\psi\right)$ and $b^{*2} = 1 - a_r^2 + a_r^2\Omega^2 / \left(\bar{a}^*[a_1 + \delta a_1]\right)^2$ .We can write G (21) at P_0 ***(Figure 2)*** as

$$G(P_0) = 4bC_1\alpha_0^2 \frac{a_1}{a_r\rho_0} \lim_{\delta a_1 \to 0} \frac{1}{2}\left(\int_{-\pi/2}^{0} + \int_{0}^{\pi/2} \right) \frac{d\psi}{\bar{a}^{*2}}$$
$$\times\Big(\alpha_2^2 - \alpha_1\left[\alpha_1(1-\nu\cos^2\psi) + \alpha_3\nu\sin 2\psi/2\right]$$
$$-\alpha_3\left[\alpha_3(1-\nu+\nu\cos^2\psi) + \alpha_1\nu\sin 2\psi/2\right]\Big) \int_{\rho_0}^{\rho_f} \frac{d\rho}{\left(1-b^{*2}\right)^{3/2}}. \qquad (33)$$

Next, we specialize the calculation to two positions $P_1(x_1' = a_1, x_3' = 0)$ and $P_2(x_1' = 0, x_3' = a_2)$ on the front of the elliptical crack lying in $Ox_1'x_3'$ with semiaxes a_1 and a_2 along x_1' and x_3'. We obtain $G_1 = G(P_1)$ and $G_2 = G(P_2)$ as

$$G_m = \frac{8\alpha_0^2}{\pi^2} G_0^I \ln\left(\frac{a_1}{\bar{a}_1}\right) \frac{1}{a_r^2}\left[\delta_{m2} + \delta_{m1}/a_r^2\right]\Big(\left[1-(1+\nu_A)\sin^2\theta - \sin 2\theta M_{12}\right]^2$$
$$-\left[\delta_{m1} + (1-\nu)\delta_{m2}\right]\left((1+\nu_A)\sin 2\theta/2 + \cos 2\theta M_{12}\right)^2$$
$$-\cos^2\theta M_{13}^2 / \left[(1-\nu)\{\delta_{m1} + (1-\nu)\delta_{m2}\}\right]\Big); \qquad (34)$$

$$M_{12} = \sigma_{21}^a / \sigma_{22}^a, \quad M_{13} = \sigma_{23}^a / \sigma_{22}^a, \quad G_0^I = K_I^{0^2}(1-\nu^2)/E, \quad K_I^0 = \sigma_{22}^a\sqrt{a_1\pi}\,.$$

The quantity in the logarithm is dimensionless, hence $\bar{a}_1$ is introduced with this respect; E is Young's modulus. We defined $< G > = (G_1 + G_2)/2$ as an average value of the crack extension force per unit length of the crack front, and

$$<\tilde{G}>=<G>/\left(G_0^I\,\frac{8\alpha_0^2}{\pi^2 a_r^4}\ln(a_1/\bar{a}_1)\right) \tag{35}$$

as a normalized quantity.

$$\begin{aligned}2<\tilde{G}>&=(1+a_r^2)\left[1-(1+\nu_A)\sin^2\theta-\sin 2\theta M_{12}\right]^2\\&-\left[a_r^2(1-\nu)+1\right]\left((1+\nu_A)\sin 2\theta/2+\cos 2\theta M_{12}\right)^2\\&-(a_r^2+1-\nu)\cos^2\theta M_{13}^2/(1-\nu)^2;\end{aligned} \tag{36}$$

$$2<\tilde{G}>(\theta=0)=1+a_r^2-\left[1+a_r^2(1-\nu)\right]M_{12}^2-(a_r^2+1-\nu)M_{13}^2/(1-\nu)^2\ .$$

The condition for an extremum of $<\tilde{G}>$ with respect to θ is given by $\partial<\tilde{G}>/\partial\theta=0$. We obtain

$$2(1-\nu)^2\partial<\tilde{G}>/\partial\theta=AM_{12}^2+BM_{12}+C \tag{37}$$

Here $A=2(1-\nu)^2\left[2+(2-\nu)a_r^2\right]\sin 4\theta$,
$B=-2(1-\nu)^2\left((1-\nu_A)(1+a_r^2)\cos 2\theta+(1+\nu_A)\left[2+(2-\nu)a_r^2\right]\cos 4\theta\right)$,
$C=-\sin 2\theta\left((1-\nu)^2(1-\nu_A^2)(1+a_r^2)\right.$
$\left.+(1-\nu)^2(1+\nu_A)^2\left[2+a_r^2(2-\nu)\right]\cos 2\theta-(a_r^2+1-\nu)M_{13}^2\right)$

For fixed M_{13}, $\partial<\tilde{G}>/\partial\theta=0$ corresponds to finding the roots of a polynomial of degree 2 in M_{12}. We obtain ($\sigma_{22}^a>0$ for tension and $\sigma_{22}^a<0$ for compression)

$$M_{12}=\text{sgn}(\sigma_{22}^a)\frac{-B+\sqrt{\Delta}}{2A}; \tag{38}$$
$$\Delta=B^2-4AC.$$

In ***Figure 3*** (***a*** and ***b)*** are exhibited $<\tilde{G}>$ (35) as a function of $M_{12}=\sigma_{21}^a/\sigma_{22}^a$ and θ the crack inclination angle (see ***Figure 1***) at $M_{13}=\sigma_{23}^a/\sigma_{22}^a=0$. For moderate fixed $|M_{12}|\leq 6$, positive maximums are observed both in tension and compression at angles 53° and 42° in tension and compression, approximately. ***Figure 4*** is a plot of the couples (M_{12}, θ) (38) at which $<\tilde{G}>$(35) exhibits extremums for fixed M_{13}. M_{12} ($\sigma_{22}^a>0$, tension) increases strongly as θ decreases to zero. The smallest positive values of M_{12} are at about 53°. The region $\theta \leq 53°$ (approximately) are associated with positive $<\tilde{G}>$ maximums. As θ increases towards 90°, M_{12} becomes negative, decreasing strongly as θ moves closer to 90°. The extremums in these θ regions are presumably minimums in tension. We should be aware that our analysis also cover compression (σ_{22}^{a} <*0* ; M_{12} < 0). Results corresponding to σ_{22}^{a} < 0 (compression) are obtained by inverting the sign of M_{12} in ***Figure 4***. In this latter situation, as θ increases towards 90°, Poisson's stress $-\nu_A \sigma_{22}^{a}$ that is tensile becomes more and more effective; this indicates that positive $<\tilde{G}>$ maximums exist above 50°.

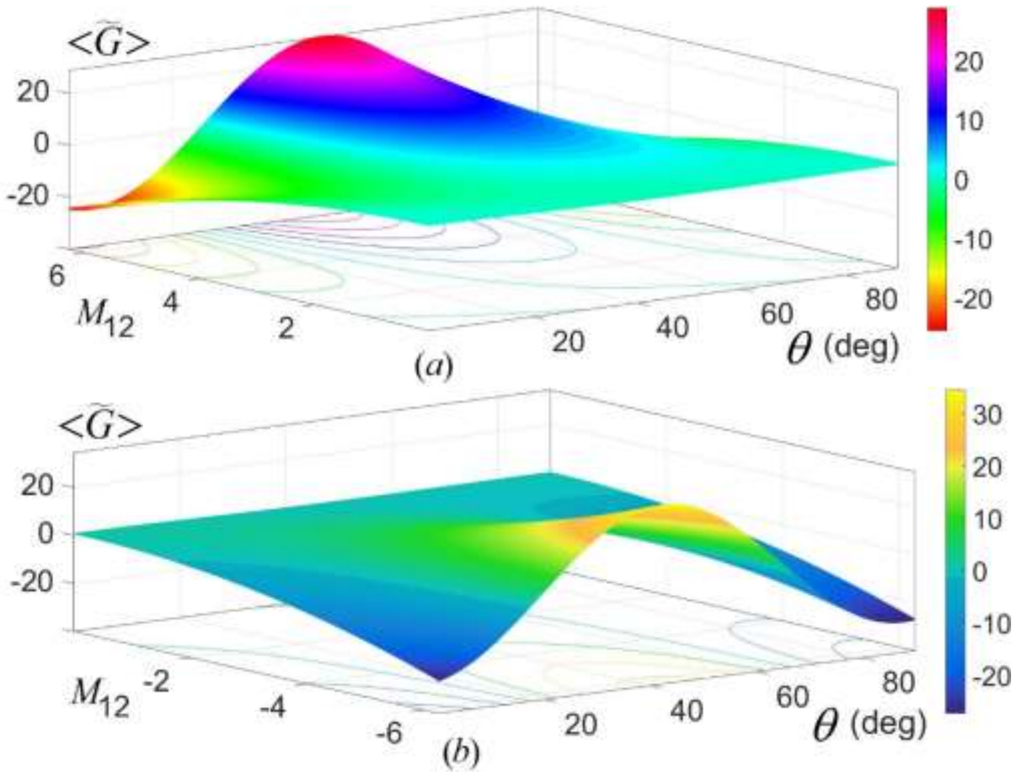

Figure 3 : *Normalized crack extension force* $<\tilde{G}>$ (35) *as a function of the reduced applied shearing stress* $M_{12} = \sigma_{21}^{a} / \sigma_{22}^{a}$ *and crack inclination angle θ. (a)* σ_{22}^{a} *> 0 for tension:* $<\tilde{G}>$ *displays positive maximums in the region about θ=53° for moderate* $M_{12} \leq 6$. *These maximums increase with* M_{12}. *(b)* σ_{22}^{a} *< 0 for compression: positive maximums* $<\tilde{G}>$ *are at about θ=42° for moderate* $|M_{12}| \leq 6$. *These maximums increase with* $|M_{12}|$. *M_{13}=0, ν=1/3 and a_r= 3/4*

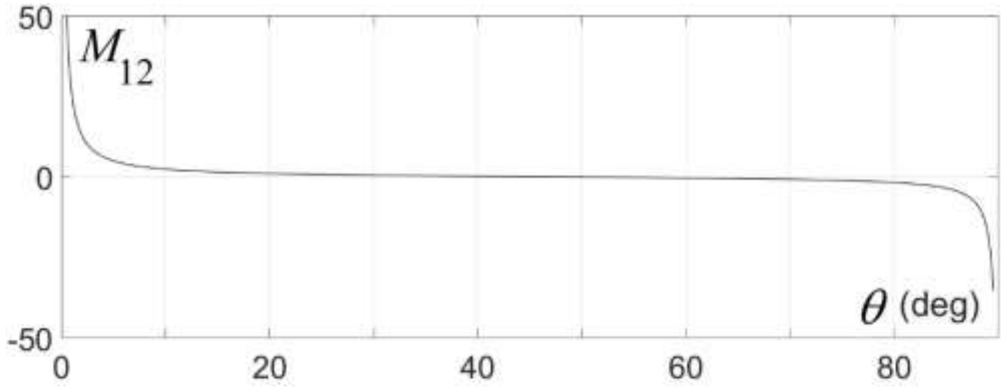

Figure 4 : *Couples (M_{12}, θ)* (38), σ_{22}^{a} *> 0 for tension, at which* $<\tilde{G}>$(35) *displays extremums when plotted against θ (at fixed M_{13}). To smaller θ correspond higher M_{12}. The positive smallest values of M_{12} are at about* 53°. *Negative values are further observed as θ moves toward* 90°. *M_{13}=0, ν=*1/3 *and a_r=* 3/4. *Results corresponding to* σ_{22}^{a} *<0 (compression) are obtained by inverting the sign of M_{12}*

IV - DISCUSSION

Approximately, one can write from (34) that $G(P_1) \approx G(P_2)/a_r^2$ for the two positions $P_1(x_1^{'} = a_1, x_3^{'} = 0)$ and $P_2(x_1^{'} = 0, x_3^{'} = a_2)$ on the front of the crack lying in $Ox_1^{'}x_3^{'}$ with semiaxes a_1 and a_2 along $x_1^{'}$ and $x_3^{'}$. $a_r = a_1 / a_2 < 1$ leads to $G_1 > G_2$; the crack expansion would begin first from P_1 and a_1 will increase towards a_2. Under such conditions, the crack evolves towards a circle (a_r = 1). We arrive at the same conclusion when a_r >1. Hence, < G > = (G_1 + G_2) / 2 is valuable as a measure of the crack extension force averaged over the length of the crack front. Another property of the crack system comes from the value of < G > at θ= 0 (36). < $\tilde{G}$ >(θ= 0) is positive under pure tension (M_{12} = 0 and M_{13}= 0) and equal to $(1+a_r^2)$. Positive < $\tilde{G}$ > indicates that the expansion of the crack corresponds to a decrease of the energy of the crack system (see [16], for example). Negative < $\tilde{G}$ > means the contrary. As can be seen from (36) at θ= 0, the shearing stresses produce negative < $\tilde{G}$ > indicating that the crack is unable to expand under pure shears parallel to the plane of the loop. This is also apparent on ***Figure 4*** that displays the couple (M_{12}, θ) at which $<\tilde{G}>$ is positive maximum in tension for θ < 53° approximately. M_{12} increases indefinitely as θ goes to zero. In support of our findings, we shall refer to Eshelby [9] who investigated the elastic fields due to an ellipsoidal inclusion (a crack is an inclusion at whose boundary there are zero surface tractions). Eshelby defined a parameter γ such that

$$\frac{\text{energy in matrix}}{\text{energy in inclusion}} = \frac{1-\gamma}{\gamma}$$

He showed that γ is about 1 for shearing stresses parallel to the plane of the loop and concluded that there is no accommodation by the matrix of the expansion of the inclusion in its own plane. In the case displayed by Eshelby [9] (see his relation (5.7), p. 393), the shearing applied stress S makes an angle α with the plane of the loop. An important implication of the observation that an elliptical crack cannot be expanded (in its own plane) under externally applied shearing stresses parallel to its plane may be that the planar elliptical crack is not the correct crack model to provide the right crack configuration that corresponds to the largest decrease of the energy of the system, under arbitrarily applied loadings. A way to get this exact configuration is to begin the crack analysis with a non-planar loop whose front should be locally of arbitrary shape, calculate the average crack extension force $< G >$ and look for crack configuration (the expected one) that maximises $< G >$. It is noticed for small positive M_{12} that positive $<\tilde{G}>$ maximums are observed at $\theta < 53°$ approximately (θ values decrease with increasing M_{12} as in ***Figure 4***). When the crack is infinitely long (under general loading mixed mode *I+II+III*), works exist that predict values of the crack inclination angle θ for positive average G maximums (see [3] and [5], as examples). Above predictions are for brittle fracture with no slip dislocations (*i.e.* plasticity). In many materials where there are both plasticity and crack initiation, an overlap is anticipated between brittle fracture prediction and maximum 45° shear direction inclination with respect to the fatigue load direction. However, situations exist where this confusion cannot be made. We shall refer to the work by Zhao et al. [18] (see their Fig. 5). The average angle of the initial fracture surface was measured as 52° with respect to the [001] far- field loading direction. This angle 52° has nothing to do with a (111)-slip plane because the angle between a [001]-direction and a (111) plane is only 35° in face-centred-cubic metals. This 52° angle observation belongs to the predictions of brittle elastic crack propagation (present analysis or [5] as a most general analysis for large cracks). Now assume that the crack inclination angle θ is close to 90° (see ***Figure 1***). Under positive σ_{22}^{a} no tension stress is applied to the crack loop. However, in compression ($\sigma_{22}^{a} < 0$), a tension $-\nu_A \sigma_{22}^{a}$ normal to the crack plane is suffered by the crack. Under such conditions, for sufficiently applied compression, a prediction can be anticipated that the crack will expand. Positive $<\tilde{G}>$ maximums should exist for angles θ closer to 90°. Lastly, we assume that

θ = 0 and no shearing stress (*i.e.* M_{12} = 0 = M_{13}). Assuming expansion of the circular crack in its own plane under pure tension, the critical stress σ_T for crack propagation is given by the Griffith $G = 2\gamma$ condition; this leads with (35) to

$$\sigma_T = \sqrt{\frac{\pi E \gamma}{4(1-\nu^2)\alpha_0^2 a_1 \ln(a_1/\bar{a}_1)}}, \quad a_r = 1 \tag{39}$$

α_0 is of the order or a fraction of 1. Its rigorous derivation requires to solve exactly the integral equations (27) for D_j. Eventually, a value to α_0 may be obtained from the expressions of the relative displacement of the faces of the crack under tension or shear as provided by different methods (see [7, 9], for example). The classical decrease of stress as the crack length increases is present in (39) except for a coefficient $\ln(a_1/\bar{a}_1)$. a_1 must be larger than $\bar{a}_1$. The physical meaning of $\bar{a}_1$ is wanted. One can speculate that the representation of the elliptical crack by continuous distributions of Volterra dislocations requires a minimum size to the crack loop.

V - CONCLUSION

An elliptical crack with center O, inside an infinitely extended isotropic elastic medium, is considered in the present study. The medium is stressed uniformly at infinity in tension σ_{22}^a along the vertical x_2 -direction and shears σ_{21}^a and σ_{23}^a (parallel to the horizontal x_1x_3- plane) in the x_1 and x_3 directions, respectively. Poisson's normal stresses $-\nu_A\sigma_{22}^a$ acting in the x_1 and x_3 directions are incorporated into the analysis. The crack is in the plane *(π)*= $Ox_1'x_3'$ tilted around $Ox_3 = Ox_3'$ by an angle θ from Ox_1x_3. The objective of the study is to analyze the conditions of expansion of this crack in its own plane. The approach used is to represent the crack by a continuous distribution of three families j (j = 1, 2 and 3) of elliptic dislocations of Burgers vectors $\boldsymbol{b}_j$ attached to the crack and oriented in the x_j' directions. The displacement and stress fields of the dislocations are first provided. The method used consists in giving the plastic distortions of the dislocations in their form in Fourier series; then by the superposition of the elastic fields due to plastic distortions of simple sinusoidal shape, one arrives at the elastic fields of the considered dislocations. The distribution functions D_j of the dislocations at equilibrium satisfy individually a singular integral equation whose expression closer to the crack front is of the simple Cauchy type; this makes it possible to give simple mathematical expressions of D_j as well as the associated relative displacement ϕ_j of the faces of the crack, crack-tip stress, and average crack extension force <*G*> per unit length of the crack front (averaged over the crack-front points). The tension stress σ_{22}^a gives a positive contribution to <*G*> suggesting that an expansion of the crack in its own plane is feasible in tension. Both shears σ_{21}^a and σ_{23}^a give a negative contribution to <*G*> when they are parallel to the crack, which indicates that an expansion of the loop is not possible under such conditions. Under general applied loading , <*G*>*(θ)* exhibits positive maximums in tension $\sigma_{22}^a > 0$ for θ less than 53° (approximately) and in compression $\sigma_{22}^a < 0$ for θ greater than 40° (approximately) the origin of which is associated with the Poisson's stress $-\nu_A \sigma_{22}^a$ which acts in tension on the crack loop. The observation that an elliptic crack cannot be expanded in its own plane under externally applied shearing stresses parallel to the plane of the loop would mean that a small planar elliptical crack is not the right configuration to dealt with crack nucleation and initiation in loaded brittle solids under general loading. We would have to begin the crack expansion study with a non-planar loop whose front is locally of arbitrary shape (thinking about an expansion into a Fourier series). Then look for the configuration that corresponds to the largest energy decrease. This is under this configuration that we should apply the Griffith condition $<G>_{max} = 2\gamma$.

REFERENCES

[1] - P.N.B. ANONGBA, An analysis of a non-planar crack under mixed mode I+III loading using infinitesimal dislocations with edge and screw average characters, *ResearchGate*, DOI: 10.13140/RG.2.2.14308.60806
[2] - P.N.B. ANONGBA, A study of the mixed mode I+III loading of a non-planar crack using infinitesimal dislocations, *Rev. Ivoir. Sci. Technol.*, 14 (2009) 55 - 86
[3] - P.N.B. ANONGBA, Non-planar crack under general loading: dislocation, crack-tip stress and crack extension force, *Rev. Ivoir. Sci. Technol.*, 16 (2010) 11 - 50
[4] - P.N.B. ANONGBA, Non-planar interface crack under general loading : III. Dislocation, crack-tip stress and crack extension force, *Rev. Ivoir. Sci. Technol.*, 32 (2018) 10 - 47
[5] - P.N.B. ANONGBA, Non-planar cracks in uniform motion under general loading, *Rev. Ivoir. Sci. Technol.*, 36 (2020) 119 - 149
[6] - M. A. SADOWSKY and E. STERNBERG, Stress concentration around a triaxial ellipsoidal cavity, *J. Appl. Mech.*, 16 (1949) 149 - 157

[7] - A. E. GREEN and I. N. SNEDDON, The distribution of stress in the neighbourhood of a flat elliptical crack in an elastic solid, *Mathematical Proceedings of the Cambridge Philosophical Society*, 46 (1950) 159 - 163
[8] - M. K. KASSIR and G. C. SIH, Three-dimensional stress distribution around an elliptical crack under arbitrary loadings, *J. Appl. Mech.*, 33 (1966) 601 - 611
[9] - J. D. ESHELBY, The determination of the elastic field of an ellipsoidal inclusion, and related problems, *Proc. Roy. Soc. A*, 241 (1957) 376 - 396
[10] - E. KRÖNER, "Kontinuumstheorie der versetzungen und eigenspannungen", Springer – Verlag, Berlin, (1958)
[11] - F. KROUPA, Circular edge dislocation loop, Czech. *J. Phys. B*, 10 (1960) 284 - 293
[12] - T. A. KHRAISHI, J. P. HIRTH, H. M. ZBIB and T. DIAZ DE LA RUBIA, The stress field of a general circular Volterra dislocation loop : analytical and numerical approaches, *Phil. Mag. Letters*, 80 (2000) 95 - 105
[13] - A. L. KOLESNIKOVA and A. E. ROMANOV, Representations of elastic fields of circular dislocation and disclination loops in terms of spherical harmonics and their application to various problems of the theory of defects, *Int. J. Solids Struct.*, 47 (2010) 58 - 70
[14] - T. MURA, The continuum theory of dislocations, In : "Advances in Materials Research" (Edited by H. Herman), Interscience Publications, Vol. 3, (1968) 1 - 108
[15] - T. MURA, "Micromechanics of defects in Solids", Martinus Nijhoff Publishers, Dordrecht (1987)
[16] - B. A. BILBY and J. D. ESHELBY, Dislocations and the theory of fracture, In : "Fracture", Ed. Academic Press (H. Liebowitz), New York, Vol. 1, (1968) 99 - 182
[17] - N. I. MUSKHELISHVILI, "Singular integral equations", Dover Publications, New York, (1992)
[18] - Z. ZHAO, F. ZHANG, C. DONG, X. YANG and B. CHEN, Initiation and early-stage growth of internal fatigue cracking under very-high-cycle fatigue regime at high temperature, *Metall. Mater. Trans. A*, 51A (2020) 1575 - 1592